

## Article

# The Impact of Curing Temperature and UV Light Intensity on the Performance of Polymer-Dispersed Liquid Crystal Devices Exhibiting a Permanent Memory Effect

Ana Mouquinho  and João Sotomayor \* 

LAQV-REQUIMTE, Department of Chemistry, NOVA School of Science and Technology, NOVA University of Lisbon, 2829-516 Caparica, Portugal; a.mouquinho@campus.fct.unl.pt

\* Correspondence: sotomayor@fct.unl.pt

**Abstract:** PDLC films, synthesized via polymerization-induced phase separation (PIPS) utilizing both temperature and UV monochromatic radiation, were derived from a blend of E7 nematic liquid crystal (LC) and PolyEGDMA875 (polyethyleneglycoldimethacrylate) oligomers, serving as the precursor for the polymeric matrix. The influence of the curing temperature on thermal polymerization, UV light intensity on photochemical polymerization, and exposure time during these processes on the electro-optical characteristics of PDLC films was thoroughly examined. Observations revealed that employing thermal polymerization during device preparation notably enhanced the permanent memory effect of the PDLC films. Sustained high transparency ( $T_{\text{OFF}} = 45\%$ ) over an extended duration at room temperature, even subsequent to voltage cessation, was achieved. This transition initiated from an opaque state ( $T_0 = 0\%$ ) through to a transparent state ( $T_{\text{MAX}} = 65\%$ ), resulting in a substantial 70% permanent memory effect.

**Keywords:** polymer-dispersed liquid crystal (PDLC); liquid crystal; permanent memory effect; photochemical polymerization; thermal polymerization



**Citation:** Mouquinho, A.; Sotomayor, J. The Impact of Curing Temperature and UV Light Intensity on the Performance of Polymer-Dispersed Liquid Crystal Devices Exhibiting a Permanent Memory Effect. *Crystals* **2024**, *14*, 571. <https://doi.org/10.3390/cryst14060571>

Academic Editors: Bouchta Sahraoui, Viviana Figà and Francesco Simoni

Received: 3 May 2024

Revised: 6 June 2024

Accepted: 17 June 2024

Published: 20 June 2024



**Copyright:** © 2024 by the authors. Licensee MDPI, Basel, Switzerland. This article is an open access article distributed under the terms and conditions of the Creative Commons Attribution (CC BY) license (<https://creativecommons.org/licenses/by/4.0/>).

## 1. Introduction

Polymer-dispersed liquid crystal (PDLC) films consist of a unique blend of nematic liquid crystals (LCs) dispersed within a solid polymer matrix. These films can be fabricated using four distinct methods: encapsulation, thermally induced phase separation (TIPS), solvent-induced phase separation (SIPS), and polymerization-induced phase separation (PIPS) [1].

The PIPS method offers a significant advantage by enabling the direct creation of a composite between glass plates coated with conductive indium tin oxide (ITO) film, eliminating the need for additional laminating procedures. This streamlined process results in the production of PDLC films in a single technological step. In the PIPS approach, phase separation of the initially homogeneous mixture and polymerization occur simultaneously. This method proved particularly well suited for our purposes due to its simplicity and the high level of control it affords over the final properties of the PDLC films [2].

PDLC exhibits the ability to transition electrically from an opaque scattering state to a highly transparent state when a film of an LC–polymer mixture is positioned between two conductive glass slides [3]. In the absence of an electric field, the liquid crystal molecules orient within each domain, albeit with random orientations across different domains. Consequently, light propagation normal to the film surface encounters a spectrum of refractive indices ranging between the ordinary refractive index ( $n_o$ ) and the extraordinary refractive index ( $n_e$ ). Due to the considerable optical anisotropy of the LC molecules employed in PDLC, the effective refractive index typically does not match that of the polymer ( $n_p$ ), leading to light scattering and rendering the PDLC opaque (OFF state). Maximizing off-state scattering necessitates a substantial birefringence ( $\Delta n = n_e - n_o$ ) [4].

Conversely, when an electric field of sufficient strength is applied across the film, overcoming interactions between the polymer matrix and liquid crystal molecules at the interfaces of LC domains–polymer matrix, the liquid crystal directors within each domain align uniformly parallel to the electric field's direction. If the ordinary refractive index of the liquid crystal matches that of the polymeric matrix ( $n_p$ ), the film becomes transparent (ON state) [5], thereby enabling the transparency of the PDLC film to be regulated by applying an electric field.

Typically, upon removal of the applied electric field, the nematic directors revert to their random distribution, causing the film to revert to an opaque state. A functional representation of a PDLC film is depicted in Figure 1.

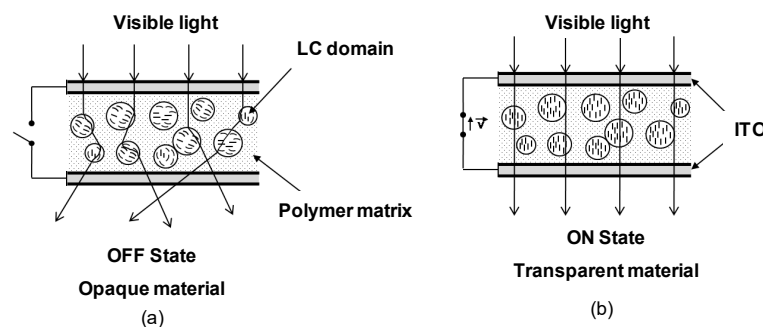


**Figure 1.** Schematic representation of the averaged molecular orientation of the liquid crystal within the microdroplets without (a) and with (b) an applied electric field.

Thanks to their electro-optic switching capabilities, PDLCs are versatile and find applications in switchable smart windows, flat-panel displays, projection systems, and sensors. PDLC devices offer several advantages, including a straightforward fabrication process that eliminates the need for alignment layers, rubbing processes, and polarizers. Additionally, they support large-scale production and the creation of flexible devices [6–9].

In specific instances, a high transparency state, termed  $T_{OFF}$ , can persist for an extended duration at room temperature, even after the applied voltage has been turned off, transitioning from an opaque state ( $T_0$ ) to a transparent state ( $T_{MAX}$ ). PDLC films exhibiting this electric-optical response demonstrate a permanent memory effect.

The permanent memory effect (PME) appears to be associated with a particular polymer matrix structure, known as the polymer ball morphology, wherein micro-sized polymer balls merge to form a network that interfaces with a continuous liquid crystal phase. In contrast, the more common polymer matrix structure involves droplet nucleation and growth, resulting in isolated liquid crystal droplets or domains surrounded by polymer separation walls, known as the Swiss cheese morphology. The polymer ball morphology facilitates collective alignment of the LC molecules, attributed to a higher surface-to-volume ratio (SVR). In contrast, in the case of isolated LC droplets, upon removal of the electric field, the LC molecules return to their initial configuration to minimize elastic free energy. However, the collective alignment in the polymer ball morphology leads to a permanent memory effect as the LC molecules maintain their orientation even after the electric field is removed [10].

Numerous variables can influence the performance of PDLC, affecting the occurrence of the permanent memory effect, with the anchoring effect being a commonly cited explanation in the literature. When the orientation of LC molecules is induced by the application of an electric field, it counteracts the anchoring effect. If this orientation persists even after the applied voltage is turned off, indicating weak interactions between LC molecules and the polymer surface, the liquid crystal remains aligned, resulting in a high transparency state without additional energy consumption [11–14].

To maximize the permanent memory effect, optimal conditions are determined to achieve the highest memory state. The switching properties of PDLC films depend on various factors, including the size and shape of LC domains, the microstructure of the

polymer network, and the molecular interactions between LC molecules and the polymer matrix. These factors, along with others, can be controlled by polymerization conditions [5]. The phase separation phenomenon between LC and polymeric matrices in PDLCs is a kinetic process wherein transport parameters play a crucial role in determining domain size and the amount of LC separated from the polymer matrix. The rate of polymerization and certain physical parameters, such as system viscosity, influence the size and shape of liquid crystal domains. These parameters are correlated with the anchoring strength at the interface between liquid crystal molecules and polymer molecules. Thus, anchoring strength not only determines the electric field required to achieve the transparent state in PDLC but also influences the level of the permanent memory effect. Several attempts have already been made by our group with PDLC systems referenced here in order to increase the PME, minimizing the switching voltage and minimizing the switching time between opaque and transparent states, relating to the type of polymerization, with the addition of additives, among others [15–18].

## 2. Materials and Methods

The liquid crystal utilized in this study was E7 (Merck, Tokyo, Japan), employed without additional purification. E7 is a complex mixture comprising three distinct cyanobiphenyls and one cyanoterphenyl in varying proportions [11,19]. Figure 2 and Table 1 illustrate the molecular structures and mass composition of the individual components constituting E7.

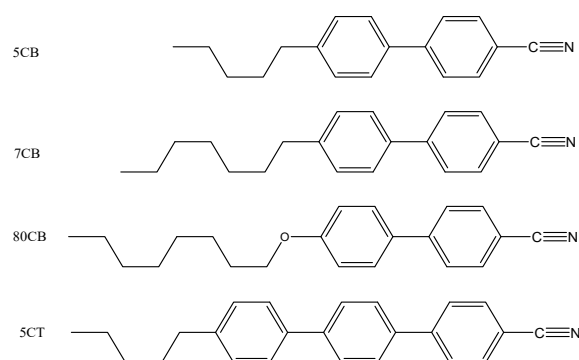


**Figure 2.** Molecular structures of the components of the nematic liquid crystal mixture E7.

**Table 1.** Components and mass composition of the nematic liquid crystal mixture E7.

Compound	Molecular Formula	IUPAC Name	Composition (w/w)	T <sub>NI</sub> (°C)
5CB	C <sub>18</sub> H <sub>19</sub> N	4-cyano-4'-pentyl-1,1'-biphenyl	51%	35.3
7CB	C <sub>20</sub> H <sub>23</sub> N	4-n-heptyl-4'-cyanobiphenyl	25%	42.8
8OCB	C <sub>21</sub> H <sub>25</sub> NO	4,4'-n-octyloxycyanobiphenyl	16%	80.0
5CT	C <sub>24</sub> H <sub>23</sub> N	4'-n-pentyl-4-cyanoterphenyl	8%	240

E7 finds extensive application in polymer-dispersed liquid crystals due to its ability to maintain anisotropic characteristics over a broad range of operating temperatures. It undergoes a nematic-to-isotropic transition at T<sub>NI</sub> = 58 °C. At room temperature, E7 exhibits a nematic phase with an ordinary refractive index (n<sub>o</sub>) of 1.5183 and an extraordinary refractive index (n<sub>e</sub>) of 1.7378, both measured at 20 °C. There are no other discernible transitions between 58 °C and −62 °C, with the latter representing a glass transition temperature [19].

The initiator utilized for thermal polymerization was N,N-azobisisobutyronitrile (AIBN), and for photochemical polymerization, it was p-xylylene bis-(N,N-diethyldithiocarbamate) (XDT). AIBN was employed as received from Sigma-Aldrich, Merck KgaA (St. Louis, MO, USA) without further purification, while XDT was synthesized following literature procedures [20]. The precursors of the polymeric matrix comprise polyethylene glycol dimethacrylate (PolyEGDMA875), sourced from Aldrich (St. Louis, MO, USA). Prior to

use, this oligomer underwent treatment with a disposable inhibitor remover column from Aldrich to eliminate the hydroquinone stabilizer.

### 2.1. Preparation of PDLC Samples

To prepare PDLC films, mixtures comprising oligomers (PolyEGDMA875) and E7 were combined at weight ratios of 30/70, along with 1% AIBN or 1% XDT by weight relative to the oligomer mixture for thermal and photochemical polymerization, respectively. The mixtures were thoroughly blended at room temperature until homogeneity was achieved. Subsequently, samples were created by capillarity, introducing the mixtures into 20  $\mu\text{m}$  ITO glass cells supplied by Instec Inc. (Boulder, CO, USA), where polymerization reactions took place directly within the ITO cell.

Thermal polymerizations were conducted using a custom-built oven equipped with an auto-tune temperature controller (CAL Controls, model CAL 3300; Farnell<sup>®</sup>, Portugal) and a resistance thermometer (Pt100/RTD-2) with a temperature range from  $-200$  to approximately  $400$  °C. The cells filled with the mixture were maintained isothermally at temperatures of 55, 60, 66, 74, 80, and 90 °C for several minutes.

For photochemical polymerizations, Oriel 60115 equipment (Oriel Instruments, Newport Corporation, Irvine, CA, USA) was employed, featuring a 100 W mercury medium-pressure lamp powered by Oriel 68800 (Oriel Instruments, Newport Corporation, Irvine, CA, USA). Samples were irradiated with monochromatic light at 366 nm using three different intensities: 0.24, 2.4, and 24  $\text{mWcm}^{-2}$ . The cells filled with the mixture were exposed to radiation for several minutes, with all photochemical polymerizations conducted at room temperature.

### 2.2. Morphology of the Polymer Network in the PDLC Films

Scanning Electron Microscopy (SEM) provided detailed images of the polymeric matrix morphology within the PDLC. To prepare samples for SEM analysis, mixtures underwent either thermal or photochemical polymerization between two KBr disks separated by 28  $\mu\text{m}$  mylar spacers. Post polymerization, these disks were immersed in water to dissolve the KBr. Subsequently, to extract the LC, samples were immersed in acetonitrile three times, followed by vacuum drying of the remaining polymer matrix for 24 h. The resulting samples were mounted on aluminum stubs using carbon cement (D-400, Neubauer Chemikalien; Agar Scientific, Essex, UK), and a thick gold coating was deposited using a dual-ion beam sputter coating apparatus. SEM imaging was conducted using a Hitachi S-2400 instrument (Hitachi, Japan) equipped with a Rontec standard energy-dispersive X-ray spectroscopy (EDS) detector.

The LC domains in PDLC films were analyzed using polarized optical microscopy (POM). POM studies were conducted using an Olympus CX31P optical polarizing microscope (Olympus Corporation, Tokyo, Japan) paired with a Mettler Toledo FP82HT hot stage (20 to 200 °C). The microstructure of the samples was observed by capturing microphotographs at appropriate temperatures, utilizing an Olympus SC-30 digital camera interfaced with a computer. Images were acquired at a magnification of 100 $\times$ . Heating and cooling runs were performed at a rate of 10 °C per minute for measurements.

### 2.3. Electro-Optical Measurements

Light transmittance studies were conducted using a diode array Avantes spectrophotometer (AvaLight-DHS and AvaSpec 2048; Avantes, Apeldoorn, Netherlands) equipped with a halogen lamp and optical fiber connections. A wavelength of 633 nm was selected for analysis. Electric pulses at 1 kHz frequency were generated using a programmable waveform generator (Wavetek 20 MHz Synthesized Function Generator Model 90, Wavetek, San Diego, CA, USA), producing an AC wave with a low amplitude ranging between 0 and 27 VRMS for sample excitation.

For electro-optical measurements, an external electric field was applied across the PDLC film. The generator, connected to a Vtrek TP-430 amplifier capable of reaching a

voltage of 47 VRMS, was linked to a 220 V/9 V transformer connected inversely, effectively multiplying the voltage by a factor of 24. A 1  $\Omega$  resistance was employed to safeguard the amplifier against short circuits, while a 150 k $\Omega$  resistance served to standardize the voltage wave output. The amplifier was powered by a Kiotto KPS 1310 power supply. The output detector (AvaSpec-2048) was connected to computer software for data acquisition.

### 3. Results and Discussion

The relationship between the shape and size of liquid crystal domains and the polymerization time of PDLC films was explored using polarized optical microscopy. Polymerization induces phase separation, driven by the limited solubility of E7 molecules within the forming polymeric matrix [1]. As depicted in Figures 3 and 4, representative results for thermal and photochemical polymerizations show that, respectively, the radii of liquid crystal domains diminish with increasing polymerization time due to crosslinking. However, this correlation is notably more pronounced in thermal polymerization.

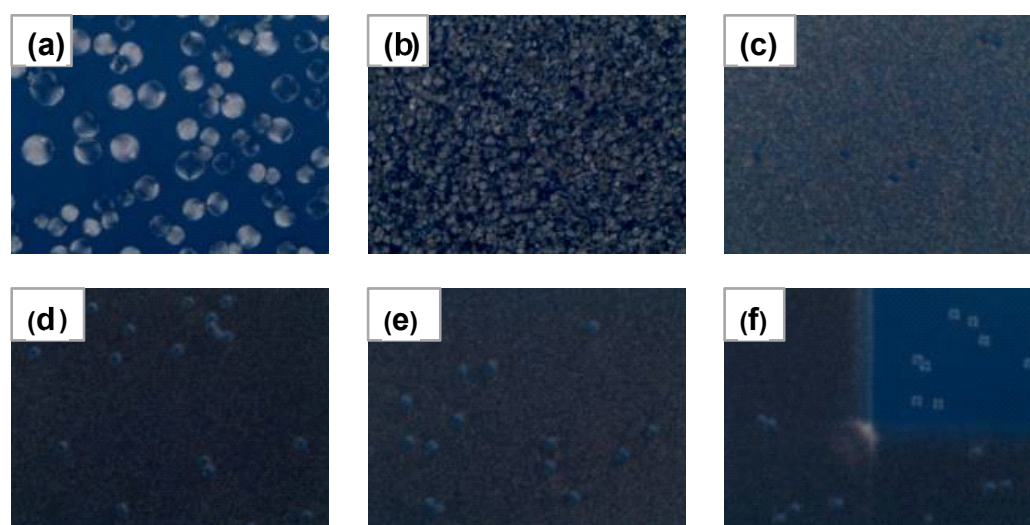


**Figure 3.** Polarized optical micrographs with crossed polarizers of PDLC films prepared with the PolyEGDMA<sub>875</sub> (1% AIBN) + E7 in a ratio of 30/70 (*w/w*) thermally polymerized at 70 °C with different polymerization times before being applied to an electric field: (a) 4 min; (b) 5 min; (c) 6 min; (d) 20 min; (e) 60 min; and (f) 60 min after being applied to the electric field and the electric field had been removed. Images were acquired at a magnification of 100 $\times$ .

Thermal polymerization proceeded at a slower rate compared to photochemical polymerization. This, coupled with the decrease in medium viscosity at higher temperatures, could potentially promote the growth of LC domains through diffusion and coalescence in the former case. However, when PDLC films were cured at elevated temperatures, the reduction in medium viscosity and the growth of LC domains might be less significant compared to the increase in the polymerization rate. Consequently, the enlargement of LC domains is strongly impeded by the accelerated polymerization rate, resulting in the formation of a high-density network and ensuring a homogeneous distribution of liquid crystal domains within the polymeric matrix (see Figure 3).

In contrast, photochemical polymerization facilitates the growth of LC domains, resulting in larger domain sizes compared to those obtained through thermal polymerization. The initiation rate in photochemical polymerization is directly proportional to the incident UV light intensity [21], and the range of UV light intensities employed appears to be sufficiently low to promote LC domain growth. This is evident in Figure 3f (bright region), where even after the electric field is removed, the LC molecules retain alignment (permanent memory effect), unlike LC molecules in photochemically polymerized PDLC films (see Figure 4f). The observations made through polarized optical microscopy (POM) were corroborated by SEM analysis. Representative micrographs of the polymer matrix

microstructure for samples subjected to thermal and photochemical polymerization are presented in Figures 5 and 6, respectively.

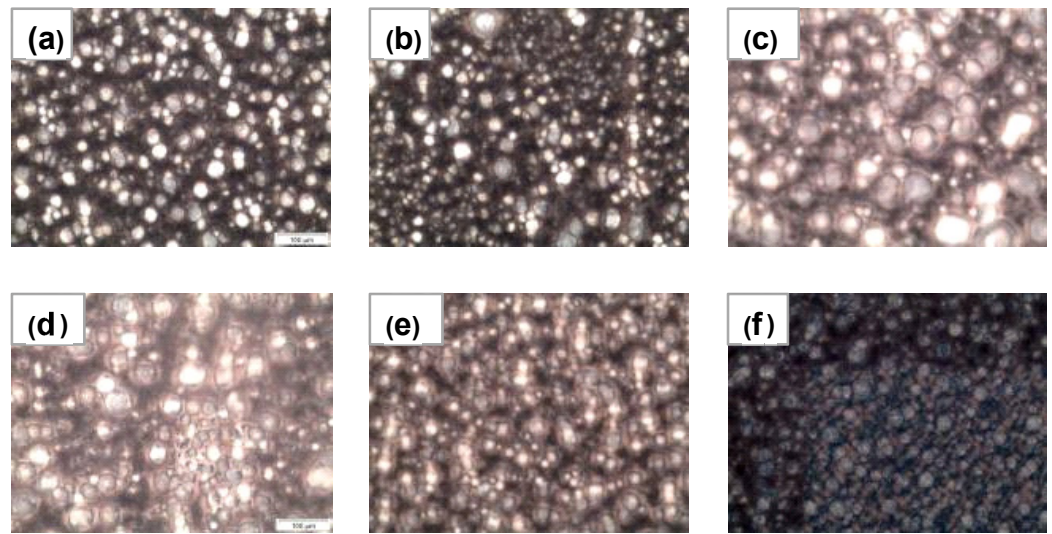


**Figure 4.** Polarized optical micrographs with crossed polarizers of PDLC films prepared with the PolyEGDMA<sub>875</sub> (1% XDT) + E7 in a ratio of 30/70 (*w/w*) photochemically polymerized at curing UV light intensity  $2.4 \text{ mWcm}^{-2}$  with different exposure times before being applied to an electric field: (a) 1000 s; (b) 1500 s; (c) 3000 s; (d) 6000 s; (e) 10,000 s; and (f) 10,000 s after being to the applied electric field and the electric field had been removed. Images were acquired at a magnification of  $100\times$ .

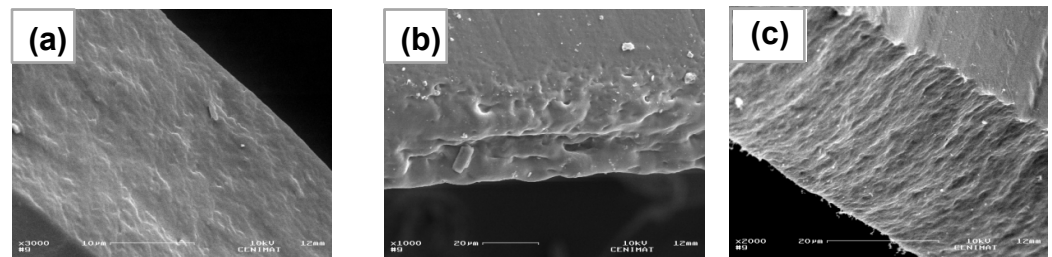


**Figure 5.** SEM micrographs for the microstructure of the polymer matrix of the PDLC films thermally polymerized at different temperatures and times: (a)  $60^\circ\text{C}$ , 90 min; (b)  $66^\circ\text{C}$ , 60 min; and (c)  $90^\circ\text{C}$ , 10 min. Images were acquired at a magnification of  $1000\times$ .

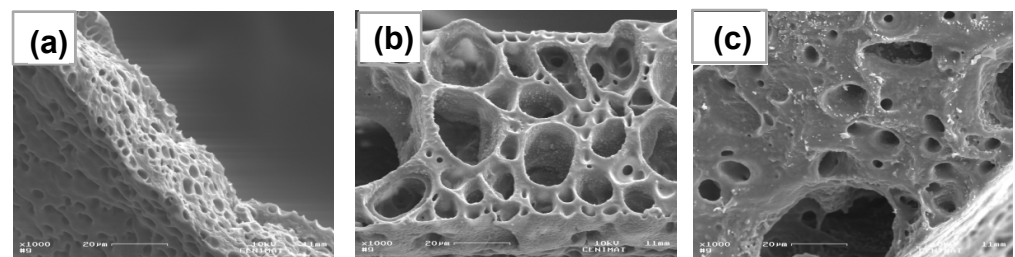


**Figure 6.** SEM micrographs for the microstructure of the polymer matrix of the PDLC films photochemically polymerized at different curing UV light intensity and times: (a)  $24 \text{ mWcm}^{-2}$ , 1500 s; (b)  $2.4 \text{ mWcm}^{-2}$ , 400 s; and (c)  $0.24 \text{ mWcm}^{-2}$ , 10,000 s. Images were acquired at a magnification of  $1000\times$ .

The microstructure of the polymer matrix depicted in Figure 5 clearly indicates that LC molecules are deeply embedded within the polymeric matrix, resulting in a reduction in the size of LC domains. Conversely, the microstructure of the polymer matrix in Figure 6 suggests a Swiss cheese morphology, where LC molecules are confined within isolated microdroplets.

The permanent memory effect (%PME) can be calculated as a percentage by

$$\%(\text{PME}) = \frac{T_{\text{OFF}} - T_0}{T_{\text{MAX}} - T_0} \times 100$$

where  $T_0$  is the transmittance for the initial opaque state (zero electric field),  $T_{\text{MAX}}$  is the maximum transmittance upon applying an electric field, and  $T_{\text{OFF}}$  is the transmittance after removing the applied field [10]. One parameter that is crucial for evaluating the efficiency of the PDLC electro-optical response is the electric field necessary to achieve 90% of the maximum transmittance, designated as  $E_{90}$ . Additionally, the memory state contrast, defined as the disparity between  $T_{\text{OFF}}$  and  $T_0$ , is reported as a percentage.

Figure 7 illustrates representative examples of the transmittance levels in PDLC films thermally polymerized at various curing temperatures, all exhibiting high memory state contrasts. Detailed information derived from electro-optical measurements is summarized in Figures 8 and 9. Notably, the memory state contrast remained approximately 55% for curing temperatures up to 74 °C but decreased to 25% for temperatures beyond this threshold.

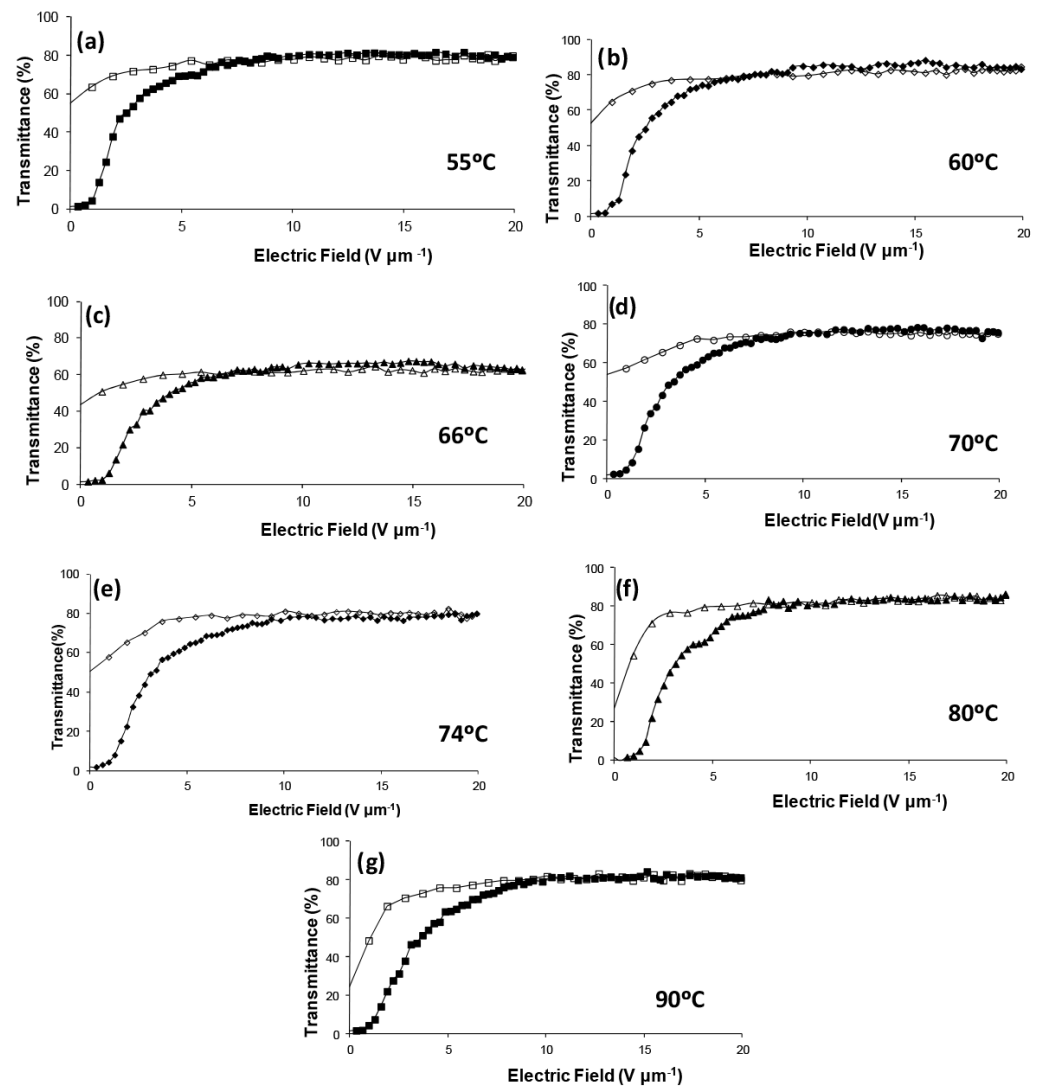


**Figure 7.** The electro-optical response optimized for PDLC films polymerized at different temperatures and times: (a) 55 °C, 120 min; (b) 60 °C, 60 min; (c) 66 °C, 60 min; (d) 70 °C, 40 min; (e) 74 °C, 20 min (f) 80 °C, 8 min; and (g) 90 °C, 6 min. The transmittance was measured by applying voltage (filled symbols) and after removing the electric field (open symbols).

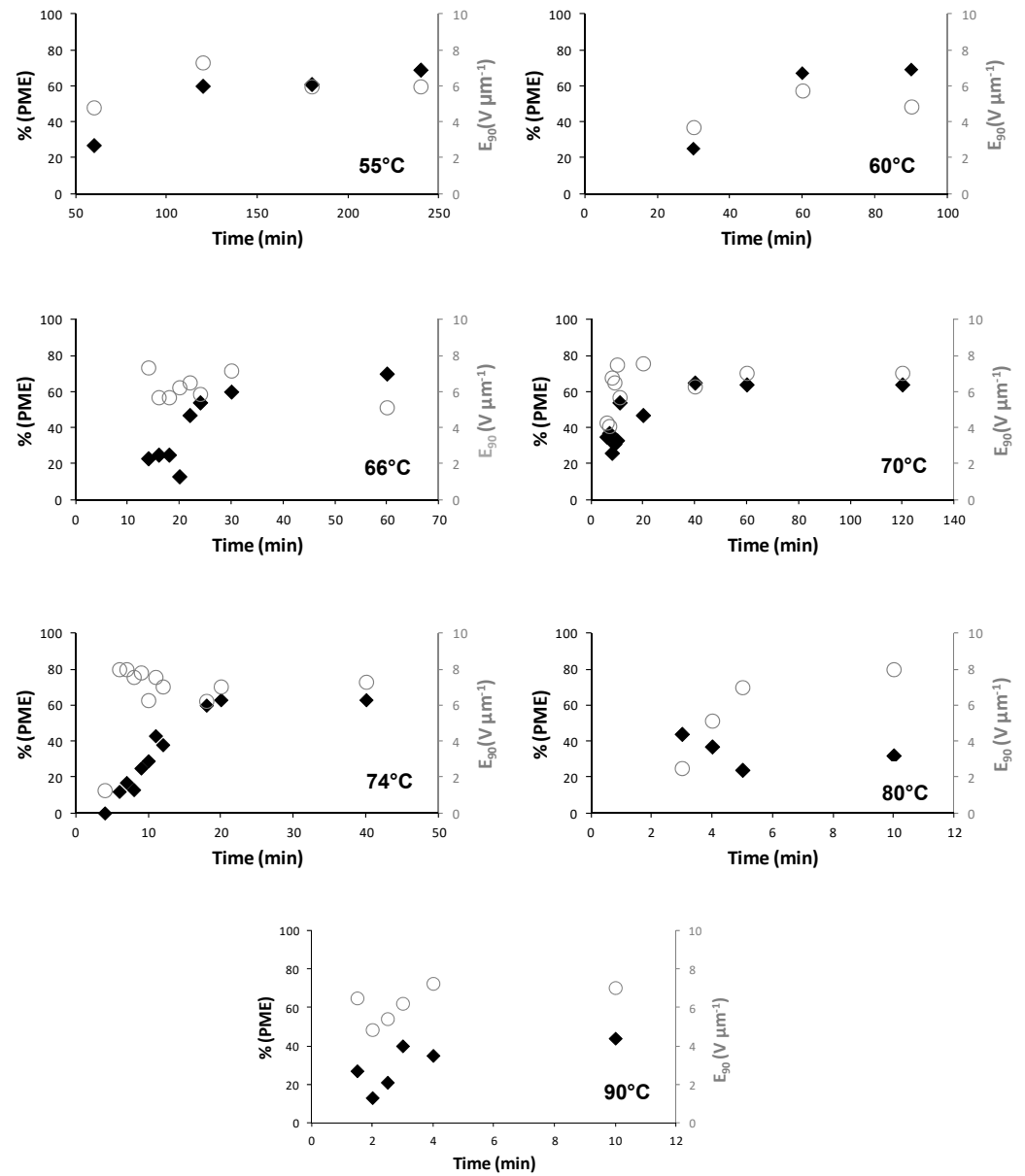


Figure 8. Values of permanent memory effect (%PME) (filled symbols) and  $E_{90}$  (open symbols) along polymerization time at different curing temperature.

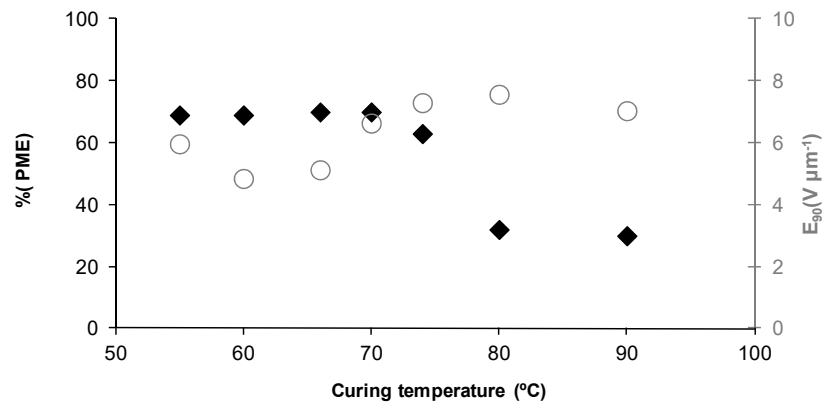
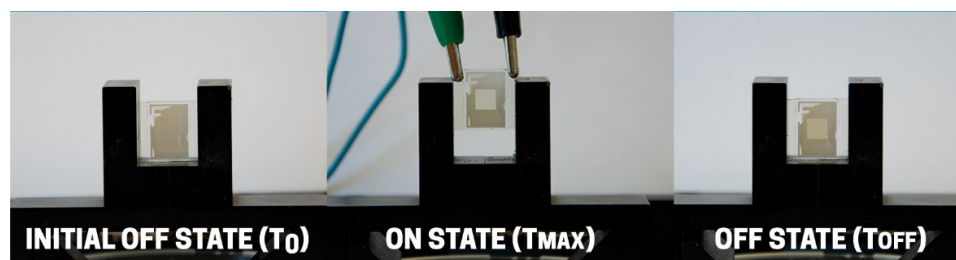


Figure 9. Summarize of the electro-optical properties of PDLC films polymerized at different temperatures, maximum %PME (filled symbols), and  $E_{90}$  (open symbols) values.

The results show a long orientation time ( $t_{90}$ , the required time to achieve 90% of maximum transmittance) of the liquid crystal molecules, around 1 ms. For this type of purpose, PME optimization, a long switching time will not be an impediment to a PDLC that is created to present an PME. The switching time depends on the nematic orientation dynamics, which mainly depends on the electric field applied to the film and the LC rotational viscosity [18]. However, the disorientation time ( $t_{10}$ , time needed to reach 10% of final transmittance after the electric field is turned off) cannot be measured due to the PME that maintains the transparency of the sample, as can be seen in Figure 10.



**Figure 10.** Example of the electro-optical response of a PDLC film with a permanent memory effect, without an electric field applied (initial OFF state), during the application of an electric field (ON state), and after the removal of an electric field (OFF state).

The permanent memory transmittance of the PDLC films thermally polymerized was found to be closely linked to both the curing temperature and polymerization time. Generally, for each curing temperature, the permanent memory effect increased with extended polymerization time until maximum phase separation was attained. The interplay between the random distribution of LC molecules and their alignment hinges significantly on the anchoring force: if weak enough, the LC molecules remain aligned even after the applied voltage is switched off. As previously mentioned, the anchoring force is intricately tied to the interactions between LC molecules and the polymeric matrix at the interface between LC domains and polymers. This dependence between the permanent memory effect and cure temperature may stem from a higher surface-to-volume ratio (SVR). PDLCs with higher SVR may exhibit weaker interactions between LC molecules and the polymer matrix [21]. Generally, the anchoring strength is inversely proportional to the SVR of PDLC films, which could explain the stronger permanent memory effect observed in thermally polymerized PDLC films.

However, at higher temperatures, such as 80 °C and 90 °C, the elevated temperature can expedite polymerization, resulting in a decrease in the amount of LC molecules separated from the polymer matrix. Consequently, the LC molecules exhibit stronger anchorage, enhancing the driving force for nematic directors to return to their random distribution after the electric field is removed. This aligns with the increased values of  $E_{90}$  with cure temperature, considering that the LC molecules are more firmly linked to the polymer matrix, and therefore, the electric field required to align them is higher.

The results for PDLC films photochemically polymerized with a Swiss cheese morphology (Figure 6) exhibited a weak permanent memory effect of less than 40% and a weak memory state contrast of around 15% for all UV light intensities, as depicted in Figures 11–13. Unlike thermally polymerized PDLCs, LC molecules in Swiss cheese morphology are confined within isolated microdomains, typically exhibiting two types of distribution: bipolar and radial configurations. These configurations are related to LC droplet size and shape and depend on whether the LC remains aligned parallel or perpendicular to the polymer surface, respectively [22]. Therefore, upon removing the applied electric field, the LC molecules in each domain revert to their initial random configuration to minimize elastic free energy [21], causing the PDLC film to become opaque again. The anchoring effect must be stronger than in the case of thermally polymerized films.

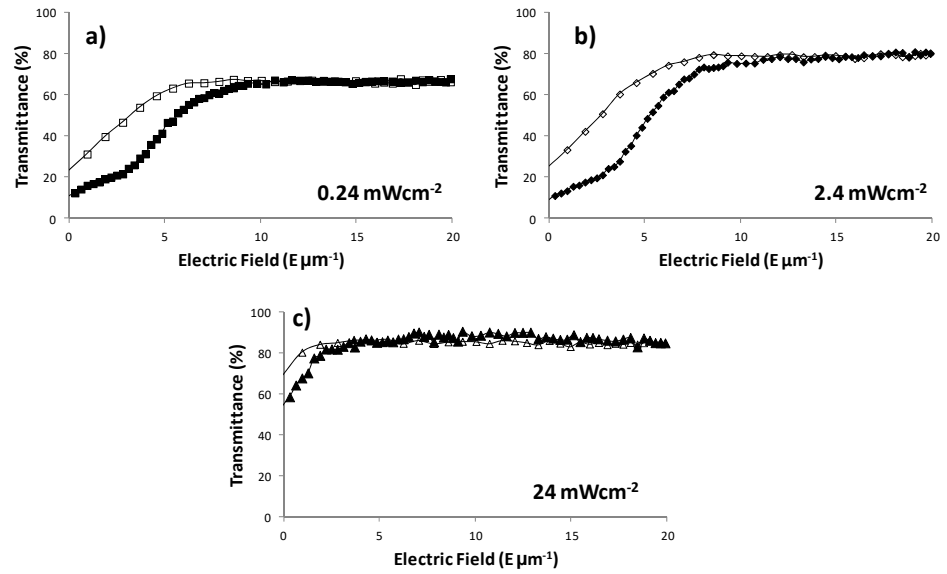


**Figure 11.** The electro-optical properties optimized for PDLC films polymerized at different curing UV light intensities and times: (a)  $0.24 \text{ mWcm}^{-2}$ , 2000 s; (b)  $2.4 \text{ mWcm}^{-2}$ , 10,000 s; and (c)  $24 \text{ mWcm}^{-2}$ , 800 s. The transmittance was measured by applying voltage (filled symbols) and after removing the electric field (open symbols).

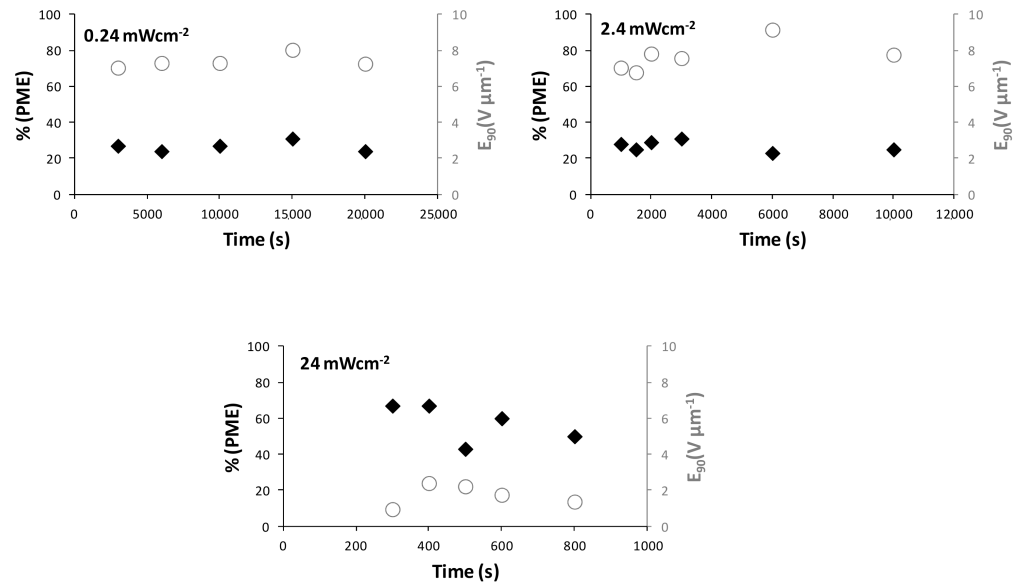


**Figure 12.** Values of permanent memory effect (%PME) (filled symbols) and  $E_{90}$  (open symbols) for each polymerization time at different UV light intensity.

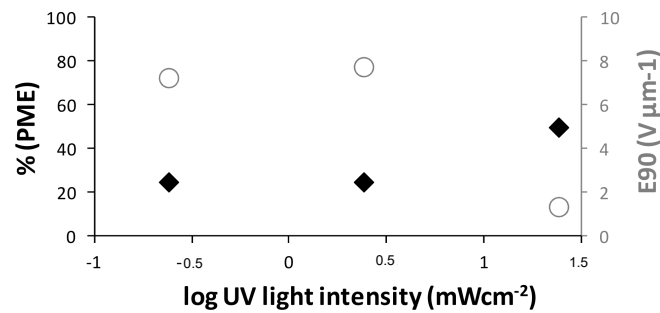


**Figure 13.** Summary of the electro-optical properties (%PME (filled symbols) and  $E_{90}$  (open symbols)) of PDLC films photochemically polymerized at different UV light intensities.

The results obtained suggest that the permanent memory effect seems to be dependent on the polymerization conditions that determine the morphology of the polymeric matrix and the amount of LC separated from the polymer network. However, previous PDLC films prepared by thermal and photochemical polymerization with a series of new monomers with structurally diverse functionalization, mimicking the structure of E7 molecules, showed a poor electro-optical response, regardless of polymerization conditions [23,24]. Therefore, the electro-optical response of PDLC films is greatly influenced not only by the polymerization conditions but also by the molecular structure of the monomers used to be incorporated as a polymeric matrix [25–27]. Moreover, the results obtained here for the permanent memory effect are higher than any reported in the literature, to our knowledge [10,14,28,29].

The molecular weight of the polymer matrix plays a crucial role in matrix morphology. Increasing the polymer molecular weight by enhancing the monomer molecular weight while maintaining the number of functionalities, such as in this study with dimethacrylates, leads to a higher network density with LC molecules embedded in the polymeric matrix [30,31]. This promotes a higher surface-to-volume ratio (SVR), which is likely to exhibit a stronger permanent memory effect. Therefore, the PolyEGDMA875 used as an oligomer in thermal polymerization for PDLC film preparation seems to be a promising candidate for achieving PDLC films with a stronger permanent memory effect.

#### 4. Conclusions

In summary, the study delved into the permanent memory effect in PDLC films, revealing that a combination of optimized polymerization conditions and the choice of monomer as a precursor of the polymeric matrix can yield a stronger memory effect. The electro-optical properties of PDLC films prepared with PolyEGDMA875 demonstrated that distinct polymerization conditions could significantly influence the permanent memory effect. Thermal polymerization, in contrast to photochemical polymerization, fosters the creation of PDLC films with a higher surface-to-volume ratio (SVR), thereby enhancing the permanent memory effect. Furthermore, thermal polymerization, coupled with an oligomer of higher molecular weight such as PolyEGDMA875, facilitated an increase in polymer chains, resulting in a denser polymeric matrix with a higher SVR.

A study of the dependence of electro-optical response on polymerization time was also conducted. The findings indicated that the performance of PDLC films with a permanent memory effect improved with prolonged polymerization time until the maximum phase separation was achieved.

Electro-optical measurements of PDLC films, prepared by blending PolyEGDMA875 with E7 in a ratio of 30/70 (*w/w*) under different polymerization conditions highlighted that devices with a permanent memory effect were optimized for thermal polymerization at temperatures ranging from 60 °C to 66 °C. Under these conditions, a remarkable 70% permanent memory effect was obtained.

**Author Contributions:** Synthesis, PDLC preparation, SEM, POM, and electro-optical characterization by A.M. and J.S.; conceptualization by J.S.; writing—original draft preparation by A.M.; writing—review and editing by J.S.; supervision by J.S. All authors have read and agreed to the published version of the manuscript.

**Funding:** This work was supported by the Associate Laboratory for Green Chemistry LAQV (UID/QUI/50006/2019) which is financed by national funds from FCT-MCTES and by FEDER funds through the COMPETE 2020 Program.

**Data Availability Statement:** The original contributions presented in the study are included in the article, further inquiries can be directed to the corresponding author.

**Conflicts of Interest:** The authors declare no conflicts of interest.

## References

1. Drazaic, P.S. *Liquid Crystal Dispersions*, 1st ed.; World Scientific Publishing: Singapore, 1995.
2. Sucheol, P.; Jin, W.H. Polymer Dispersed Liquid Crystal Film for Variable-Transparency Glazing. *Thin Solid Film.* **2009**, *517*, 3183–3186.
3. Benkhalel, L.; Coqueret, X.; Traisnel, A.; Maschke, U.; Mechernene, L.; Benmouna, M. A Comparative Study of UV and EB-Cured PDLC Films via Electro-Optical Properties. *Mol. Cryst. Liq. Cryst.* **2004**, *412*, 477–483. [[CrossRef](#)]
4. Vaz, N.A.; Montgomery, G.P. Refractive indices of polymer-dispersed liquid crystal film materials: Epoxy based systems. *J. Appl. Phys.* **1987**, *62*, 3161–3172. [[CrossRef](#)]
5. Nomura, H.; Suzuki, S.; Atarashi, Y. Electrooptical Properties of Polymer Films Containing Nematic Liquid Crystal Microdroplets. *Jpn. J. Appl. Phys.* **1990**, *29*, 522–528. [[CrossRef](#)]
6. Hemaida, A.; Ghosh, A.; Sundaram, S.; Mallick, T.K. Evaluation of thermal performance for a smart switchable adaptive polymer dispersed liquid crystal (PDLC) glazing. *Sol. Energy* **2020**, *195*, 185–193. [[CrossRef](#)]
7. Bronnikov, S.; Kostromin, S.; Zuev, V. Polymer-dispersed liquid crystals: Progress in preparation, investigation, and application. *J. Macromol. Sci. Part B Phys.* **2013**, *52*, 1718–1735. [[CrossRef](#)]
8. Lai, Y.T.; Kuo, J.C.; Yang, Y.J. Polymer-dispersed liquid crystal doped with carbon nanotubes for dimethyl methylphosphonate vapor-sensing application. *Appl. Phys. Lett.* **2013**, *102*, 191912. [[CrossRef](#)]
9. Sheraw, C.D.; Zhou, L.; Huang, J.R.; Gundlach, D.J.; Jackson, T.N.; Kane, M.G.; Hill, I.G.; Hammond, M.S.; Campi, J.; Greening, B.K.; et al. Organic thin-film transistor-driven polymer-dispersed liquid crystal displays on flexible polymeric substrates. *Appl. Phys. Lett.* **2002**, *80*, 1088–1090. [[CrossRef](#)]
10. Han, J. Study of Memory Effects in Polymer Dispersed Liquid Crystal Films. *Korean J. Phys. Soc.* **2006**, *49*, 1482–1487.
11. Bedjaoui, L.; Gogibus, N.; Ewen, B.; Pakula, T.; Coqueret, X.; Benmouna, M.; Maschke, U. Preferential Solvation of the eutectic mixture of liquid crystal E7 in a polysiloxane. *Polymer* **2004**, *45*, 6555–6560. [[CrossRef](#)]
12. Amundson, K.; Blaaderen, A.V.; Wiltzius, P. Morphology and electro-optic properties of polymer-dispersed liquid-crystal films. *Am. Phys. Soc.* **1997**, *55*, 1646–1654. [[CrossRef](#)]
13. Andy FY, G.; Tsung, C.K.; Mo, H.L. Polymer Dispersed Liquid crystal Films with memory characteristics. *J. Appl. Phys.* **1992**, *31*, 3366–3369.
14. Yamaguchi, R.; Sato, S. Highly transparent memory states by phase transition with a field in polymer dispersed liquid crystal films. *Jpn. J. Appl. Phys.* **1992**, *31*, 254–256. [[CrossRef](#)]
15. Mouquinho, A.; Barros, M.T.; Sotomayor, J. Pre-Polymer Chain Length: Influence on Permanent Memory Effect of PDLC Devices. *Crystals* **2024**, *14*, 249. [[CrossRef](#)]
16. Mouquinho, A.; Figueirinhas, J.L.; Sotomayor, J. Digital Optical Memory Devices based on Polymer Dispersed Liquid Crystals Films: Appropriate polymer matrix morphology. *Liq. Cryst.* **2020**, *47*, 636–649. [[CrossRef](#)]
17. Mouquinho, A.; Corvo, M.C.; Almeida, P.L.; Feio, G.M.; Sotomayor, J. Influence of Chain Length of pre-Polymers in Permanent Memory Effect of PDLC assessed by solid-state NMR. *Liq. Cryst.* **2020**, *47*, 522–530. [[CrossRef](#)]
18. Silva, M.C.; Figueirinhas, J.L.; Sotomayor, J. Effect of an additive on the Permanent Memory Effect of Polymer Dispersed Liquid Crystal Films. *J. Chem. Technol. Biotechnol.* **2015**, *90*, 1565–1569. [[CrossRef](#)]
19. Brás, A.R.; Henriques, S.; Casimiro, T.; Ricardo, A.A.; Sotomayor, J.; Caldeira, J.; Santos, C.; Dionísio, M. Characterization of a Nematic Mixture by Reversed-Phase HPLC and UV Spectroscopy: Application to Phase Behavior Studies in Liquid Crystal CO<sub>2</sub> Systems. *Liq. Cryst.* **2007**, *34*, 591–597. [[CrossRef](#)]
20. Otsu, T.; Kuriyama, A. Living mono- and biradical polymerizations in homogeneous system synthesis of AB and ABA type block copolymers. *Polym Bull.* **1984**, *11*, 135–142. [[CrossRef](#)]
21. Li, W.; Cao, Y.; Kashima, M.; Kong, L.; Yang, H.J. Effects of the structures of polymerizable monomers on the electro-optical properties of UV cured polymer dispersed liquid crystal films. *Polym. Sci. Part B Polym. Phys.* **2008**, *46*, 1369–1375. [[CrossRef](#)]
22. Collings, P.J. *Liquid Crystals: Nature's Delicate Phase of Matter*, 2nd ed.; Princeton University Press: Princeton, NJ, USA, 2002.
23. Barros, M.T.; Mouquinho, A.; Petrova, K.; Saavedra, M.; Sotomayor, J. Fast synthesis employing a microwave assisted neat protocol of new monomers potentially useful for the preparation of PDLC films. *Cent. Eur. J. Chem.* **2011**, *9*, 557–566.
24. Mouquinho, A.; Saavedra, M.; Maiau, A.; Petrova, K.; Barros, M.T.; Figueirinhas, J.L.; Sotomayor, J. Films Based on New Methacrylate Monomers: Synthesis, Characterisation and Electro-optical properties. *Mol. Cryst. Liq. Cryst.* **2011**, *542*, 132/[654]–140/[662]. [[CrossRef](#)]
25. Bulgakova, S.A.; Mashin, A.I.; Kazantseva, I.A.; Kashtanov, D.E.; Jones, M.M.; Tsepkov, G.S.; Korobkov, A.V.; Nezhdanov, A.V. Influence of the Composition of the Polymer Matrix on the Electrooptical Properties of Films with a Dispersed Liquid Crystal. *Russ. J. Appl. Chem.* **2008**, *81*, 1446–1451. [[CrossRef](#)]
26. He, J.; Bin, Y.; Wang, X.; Yu, B.; Wang, Y. A novel Polymer dispersed Liquid Crystal film prepared by reversible addition fragmentation chain transfer polymerization. *Eur. Polym. J.* **2007**, *43*, 4037–4042. [[CrossRef](#)]
27. Ahmad, F.; Jamil, M.; Jeon, Y.J.; Woo, L.J.; Jung, J.E.; Jang, J.E.; Lee, G.H.; Park, J.J. Comparative study on the electrooptical properties of polymer-dispersed liquid crystal films with different mixtures of monomers and liquid crystals. *Appl. Polym. Sci.* **2011**, *121*, 1424–1430. [[CrossRef](#)]
28. Torgova, S.I.; Dorozhkina, G.N.; Novoseletskii, N.V.; Umanskii, B.A. Investigation of memory effect in dichroic dyes based PDLC films. *Mol. Cryst. Liq. Cryst.* **2004**, *412*, 513–517. [[CrossRef](#)]

29. Yamaguchi, R.; Sato, S. Memory effects of light transmission properties in Polymer-Dispersed-LiquidCrystal (PDLC) films. *Jpn. J. Appl. Phys.* **1991**, *30*, 616–618. [[CrossRef](#)]
30. Yan, B.; He, J.; Du, X.; Qin, A.; Zhang, Q.; Wang, Y.J. Effect of molecular weight of macro-iniferter on electro-optical properties of polymer dispersed liquid crystal films prepared by iniferter polymerization. *Polym. Sci. Part B Polym. Phys.* **2009**, *47*, 1530–1534. [[CrossRef](#)]
31. He, J.; Yan, B.; Yu, B.; Wang, S.; Zeng, Y.; Wang, Y. The effect of molecular weight of polymer matrix on properties of polymer-dispersed liquid crystals. *Eur. Polym. J.* **2007**, *43*, 2745–2749. [[CrossRef](#)]

**Disclaimer/Publisher’s Note:** The statements, opinions and data contained in all publications are solely those of the individual author(s) and contributor(s) and not of MDPI and/or the editor(s). MDPI and/or the editor(s) disclaim responsibility for any injury to people or property resulting from any ideas, methods, instructions or products referred to in the content.